

A differential scanning calorimeter study of Mg-Al-Ca ternary system

X.Wang¹, M.A. Parvez¹, E.Essadiqi² and M.Medraj¹

¹Concordia University, Montreal, Canada, mmedraj@me.concordia.ca

²CANMET-MTL, Ottawa, Canada, essadiqi@NRCan.gc.ca

The ternary phase diagram for Mg-Al-Ca alloy system is investigated experimentally on the basis of a quantitative analysis using Differential Scanning Calorimeter (DSC). Experiments mainly focused on magnesium-rich corner. DSC measured endothermic and exothermic processes in materials as a function of temperature. Interpretations of the DSC spectra corresponding to this system are presented.

1. INTRODUCTION

Magnesium is the lightest metallic material used for structural applications with a density of 1.741g/cm^3 in comparison with the densities of Al (2.70g/cm^3) and Fe (7.86g/cm^3). Magnesium also has the best strength to weight ratio of common structural metals and has exceptional die-casting characteristics [1-3]. This makes magnesium alloys are one of the most promising light-weight materials for automotive applications. The current use of Mg in automotive application is limited to non-critical parts because of its restricted creep properties. When the temperature is increased, strength becomes strongly time-dependent and loads which caused no permanent deformation at room temperature cause slow and continuous deformation with time. Hence magnesium faces a challenge in meeting the performance requirements of the components, which operate at elevated temperature.

Magnesium alloys, which are used commercially, contain Al and Zn. Rare earth metals can be added to improve creep resistance of these alloys by forming precipitates [4]. Some attempts were made in the last decades to replace the rare earths metals by Ca. Calcium additions for improvement of the creep properties offer several additional advantages comparing to the cost intensive rare earths additions.

Pekguleryuz *et al.* [5] showed that die-casted Mg-Al-Ca alloys offer creep resistance, tensile strength and corrosion resistance which are comparable to commercially used Mg-alloys with rare earth additions such as AE42. Figure 1 shows a comparison between creep deformation of Mg-Al-Ca and two commercial alloys. Since the stability of Al_2Ca precipitates is comparable to the rare earth precipitates, creep resistance can be achieved using Ca with much lower costs [4]. Al_2Ca is generally present along the grain boundary in the die-cast microstructure. It is likely that this thermally stable phase at grain boundaries impedes grain boundary sliding and diffusion-related dislocations climb at high temperatures. The Al_2Ca phase has a high melting point (1079°C) and thus results in metallurgical stability of the grain boundaries at the elevated temperature. Tensile strength and impact toughness by Ca addition to the most commonly used AZ91 are also improved.

Pekguleryuz *et al.* [5] also pointed out that the absence of $\text{Mg}_{17}\text{Al}_{12}$ intermetallic in Mg-Al-Ca alloys and any aging and creep-induced precipitation in the alloy structure prevents creep.

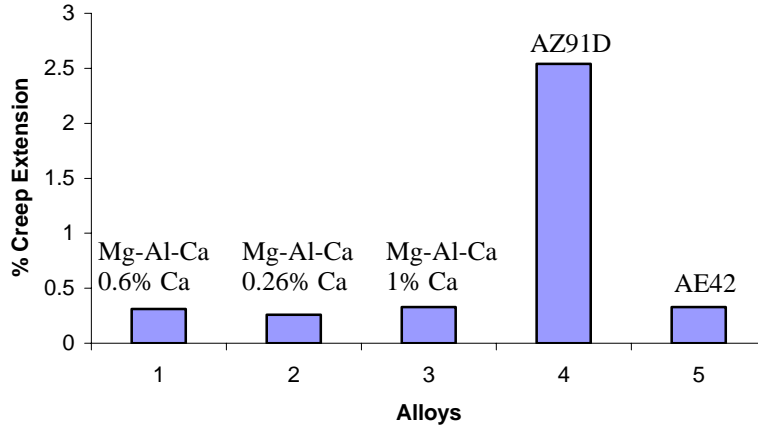


Figure 1: Comparison of creep resistance at 150°C, 35 MPa for 200 hrs [5].

Although Mg-Al-Ca alloys have great potential in automobile and aerospace industries, the phase diagram, which is very essential for process development such as casting, forging, heat treatment, etc. is scarcely known.

To date, there is little information on the Mg-Al-Ca ternary system available in the literature. Koray *et al.* [6] carried out an investigation on the phase identification and microanalysis in the Mg-Al-Ca alloy system using X-ray diffraction (XRD) and energy dispersive X-ray spectroscopy (EDS) technique. In the work of Gröbner *et al.* [4], thermodynamic calculation of ternary Mg-Al-Ca phase diagram was performed based on the three binary subsystems whereas experimental investigations were carried out by DTA and X-ray powder diffraction analysis. Zhong *et al.* [7] calculated the ternary Mg-Al-Ca diagram by combining the data of the three binary systems, Al-Mg, Ca-Mg, and Al-Ca, assuming no ternary solubility in the binary compounds along with no ternary interactions. Recent investigations pointed out that Al₂Ca and CaMg₂ are the primary precipitates responsible for the improvement of creep resistance in this system [8]. However, the composition ranges for formation of these precipitates differ drastically from one researcher to another. For instance, Gröbner *et al.* [4] reported that it is possible to form CaMg₂ with up to 32 at% Al, whereas Zhong *et al.* [7] reported only up to 18 at% Al. A considerable discrepancy among the published results and very few experimental data demands new investigation on this system.

The main intent of this research is to obtain reliable ternary phase diagram system through thermal analysis experiments combined with thermodynamic modeling. However, this paper focuses primarily on the thermal analysis using Differential Scanning Calorimeter (DSC), which will provide important thermophysical information for the reassessment of the phase diagram.

2. EXPERIMENTAL

Thermal analysis was performed using Setaram Setsys DSC-1200 apparatus. The experimental conditions used for the analysis are presented in Table 1.

Mg-samples are highly reactive with platinum and also affected the internal alumina crucibles. In addition, the highly reactive Mg-alloys oxidize easily in solid state. Melting range, starting below 600°C, is usually accompanied with a noticeable mass loss [9].

To prevent chemical reactions with Mg vapors, graphite crucibles are used. In addition, sample masses are reduced and the crucibles are covered by graphite lid. The heating rate 5°C/min is chosen to minimize the retention time during liquid phase. All the tests were carried out in a flowing argon atmosphere. To avoid oxidation, multiple evacuating followed by rinses with argon was done.

Table 1: Experimental conditions for the determination of thermophysical properties

Item	Conditions
Heating rate	5°C/min
Cooling rate	5°C/min
Temperature range	25-800°C
Inert gas	Flowing argon
Weight of sample	40~50 mg

Thirty samples were chosen by critical assessment of the experimental and thermodynamic datasets available in the literature. Special attention was directed to Mg-rich corner because of the interest in the Mg alloys, as given in Figure 2. However, in this paper, only eight samples (position located in black circles) are discussed.

The alloys were of high purity with the nominal compositions given in Table 2. In preparing the

alloys, magnesium of 99.8 wt%, aluminum of 99.9 wt.% and calcium of 99 wt.% were used. The charge was melted in a graphite crucible in an induction melting furnace under argon with 1% SF₆ to protect the melt from oxidation.

Temperature calibration of the DSC equipment was done using standard samples of Al since its melting point is similar to Mg-alloys.

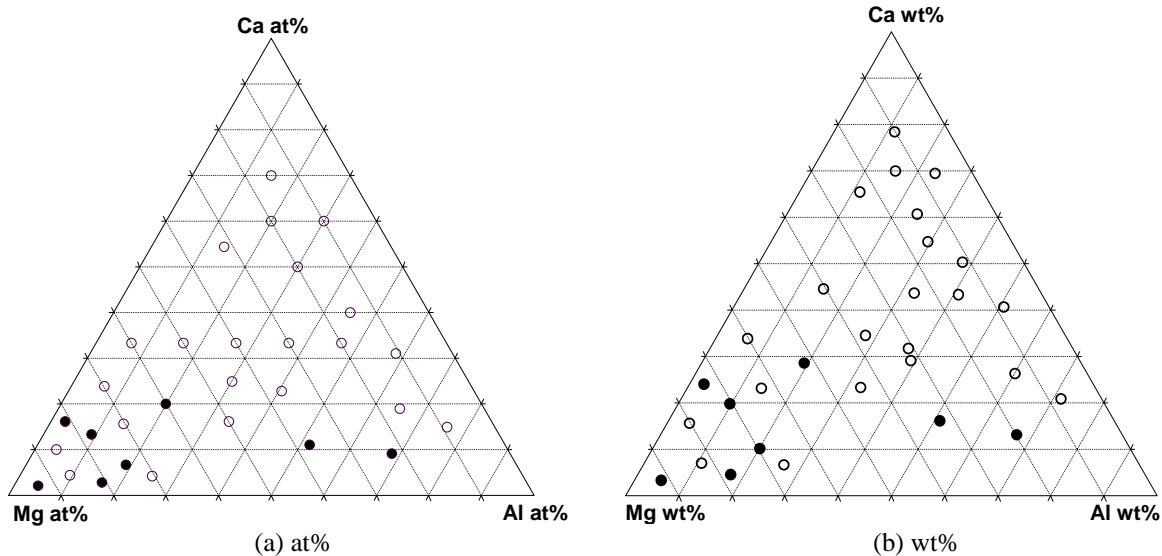


Figure 2: Mg-Al-Ca phase diagram with the investigated compositions (a) atomic % and (b) weight %.

Table 2: Nominal composition of the studied alloys.

Sample number	at.% of Ca	at.% of Mg	at.% of Al
1	6.47	74.33	19.20
2	2.83	80.84	16.33
3	9.08	22.46	68.46
4	16.12	81.18	2.70
5	19.97	60	20.03
6	11.1	36.93	51.96
7	13.23	79.60	9.57
8	2.04	93.38	4.58

The samples were cut and mechanically polished to remove any possible contaminated surface layers. After that it was cleaned with acetone and placed in a graphite crucible and covered with a lid. DSC's furnace was evacuated and purged with argon three times before heating started. Samples are heated and cooled under flowing argon with the experimental conditions mentioned above. The reproducibility of every measurement was confirmed by collecting the data during three heating and cooling cycles. The estimated error of measurements between the repetitive heating is $\pm 1^\circ\text{C}$ or less. Furthermore, difference between heating and cooling peaks was in most cases lower than 15°C .

Temperatures along with enthalpy corresponding to various thermal events were obtained from the analysis of the DSC curve. In this paper, for the analysis of DSC thermograms, both endothermic and exothermic spectra are used.

3. RESULTS AND DISCUSSIONS

Figure 3 shows the DSC spectrum of sample 1 with thermal data during heating scan. It shows a sharp melting at 526°C . The enthalpy of melting is registered as 387.6 J/g . Peaks associated with endothermic process are plotted downwards. Figure 4 shows the DSC spectrum of sample 1 during cooling run. The onset temperature during cooling was about 16°C below the onset temperatures observed in the heating process.

The onset temperature and enthalpy of this sample was calculated without the subtraction of the baseline. Onset temperatures for the melting were obtained from the points of intersection of extrapolated baseline and the line of maximum slope. The temperature corresponding to the tail ends gives the liquidus temperature, which is 560°C . This sample is very close to eutectic composition as no shoulders or any other heat effects are detected after 1st endotherm/exotherm.

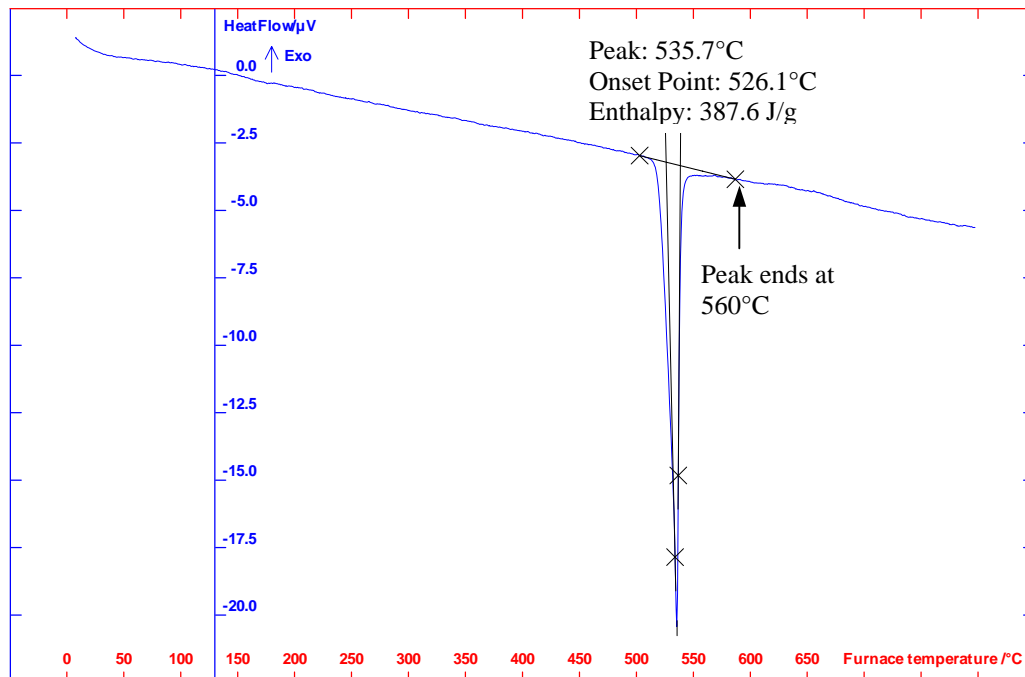


Figure 3: DSC curve of sample 1 with integration of phase change peaks during heating

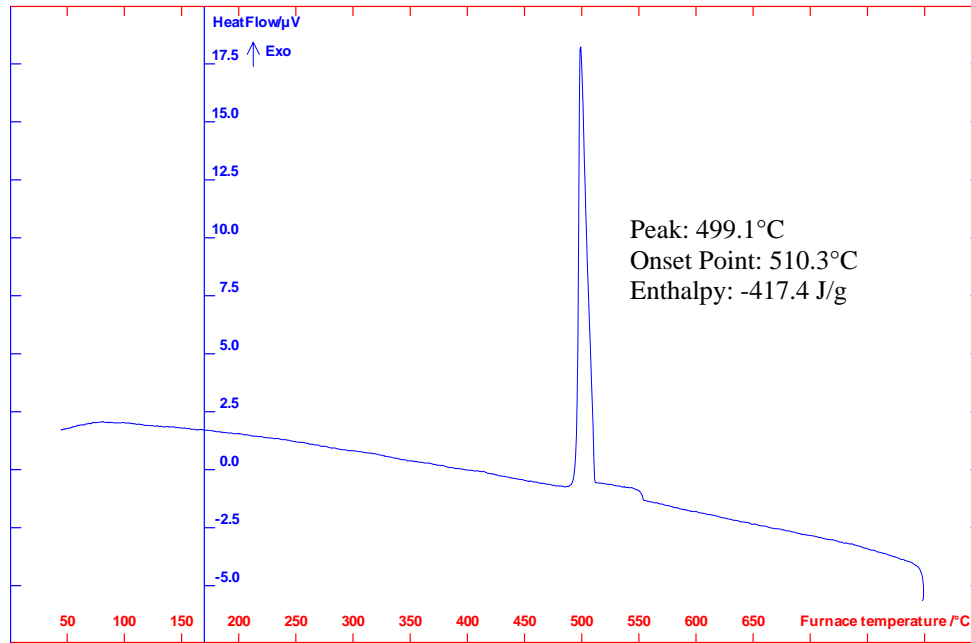


Figure 4: DSC curve of sample 1 with integration of phase change peaks during cooling.

DSC spectrum of sample 2 is plotted in Figure 5. There are two thermal events being observed in the spectrum. The first peak is sharp and narrow, which is supposed to be an isothermal transition. The heat capacity is infinite in this phase. Table 3 summarizes the parameters of melting for the eight Mg-Al-Ca samples. The composition of this sample is very close to one of the samples investigated by Tkachenko *et al.* [8] using DTA. They reported four phase transformations at 450°C, 490°C, 525°C and 555°C. On the other hand, the present investigation registered the

transformations at 444°C, 465°C, 506°C and 560°C with two predominant endothermic peaks. There is a discrepancy in second transformation temperature, which is due to the overlapping of the peaks. The reported temperature range by Tkachenko *et al.* [8] where the phase transformations occurred is quite similar to this study. The liquidus temperature observed here is 5°C higher than the liquidus temperature reported by [8].

Table 3: Parameters of melting for the eight samples.

Sample	Sample 1	Sample 2	Sample 3	Sample 4	Sample 5	Sample 6	Sample 7	Sample 8
Onset Temp. °C (Peak 1)	526.08	443.03	450.29	445.37	522.3	519.61	554.82	465.63
Enthalpy J/g (Peak 1)	387.6	189.6	-136.3	-41.1	353.6	268.7	772.1	212.1
Onset Temp. °C (Peak 2)	-	505.8	504.87	521.32	-	-	628.20	-
Enthalpy of melting J/g	-	197.4	-94.5	-331.8	-	-	99.6	-
Liquidus Temp. °C	560	560	640	570	575	562	660	680

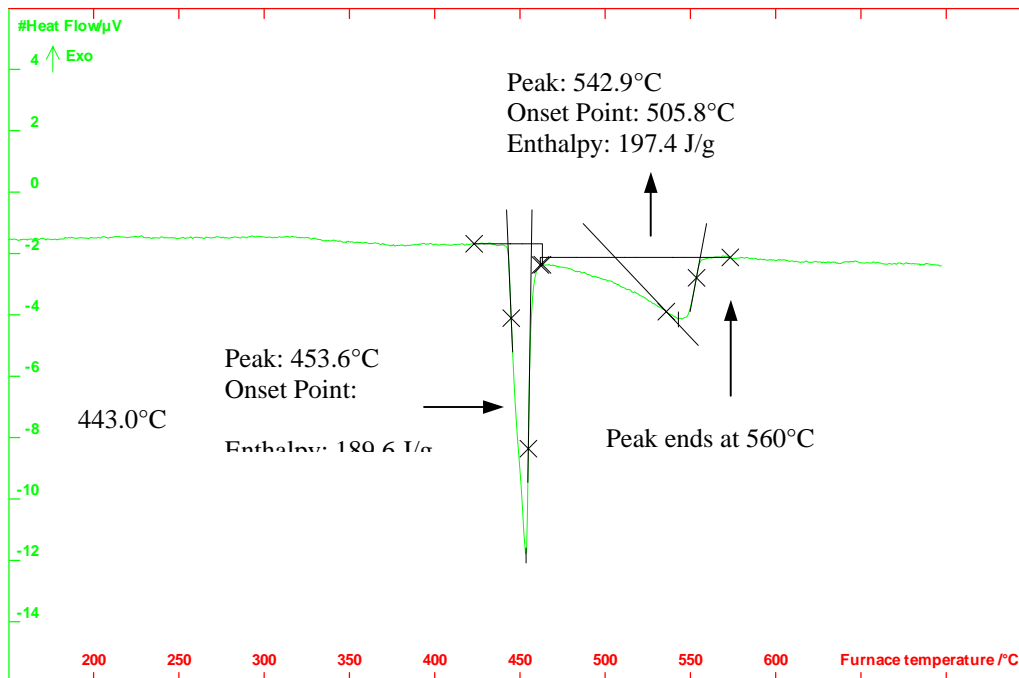


Figure 5: DSC curve of sample 2 with integration of phase change peaks.

Figure 6 shows the DSC spectrum of sample 3. It shows two peaks during cooling. These results are reproduced three times. The cooling runs are taken into consideration here as due to favorable kinetics. The enthalpy and onset temperatures were found after the baseline subtraction and by using horizontal plot. In this sample, the tailing

of the 1st exothermic peak appears at 640°C, which corresponds to liquidus temperature. This peak is lower and broader and indicates univariant transition. Here the peaks also overlap each other.

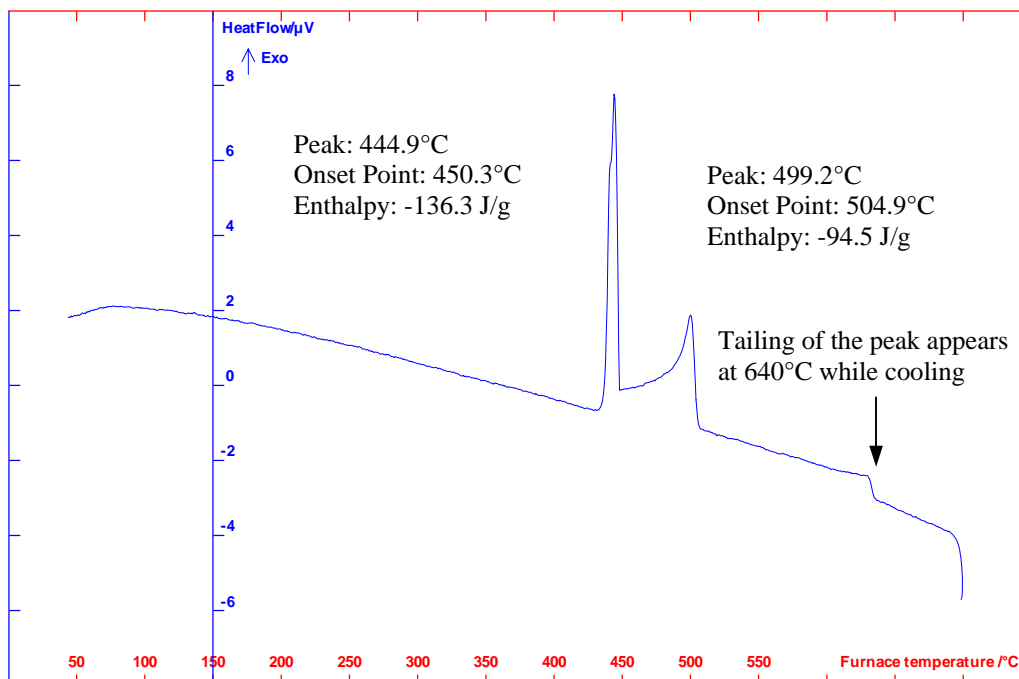


Figure 6: DSC curve of sample 3 with integration of phase change peaks.

Figure 7 shows the DSC spectrum of sample 4. In this composition, two predominant exothermic peaks were revealed during cooling, one starting at 445°C and another at 521°C. The peak at 440°C is sharp and narrow, which corresponds to the infinite heat capacity change during the

transformation and corresponds to eutectic reaction. The absence of a single exothermic peak without any tail indicates that the sample does not melt congruently. It is supposedly undergoes a peritectic decomposition. The tail of the peak returns to the baseline at 570°C.

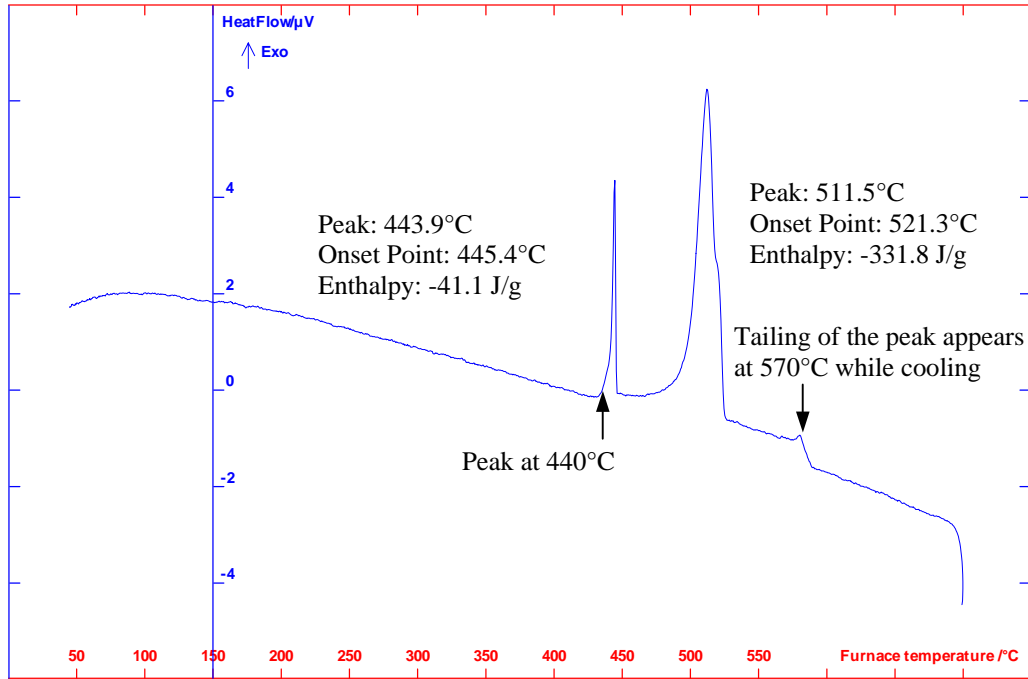


Figure 7: DSC curve of sample 4 with integration of phase change peaks.

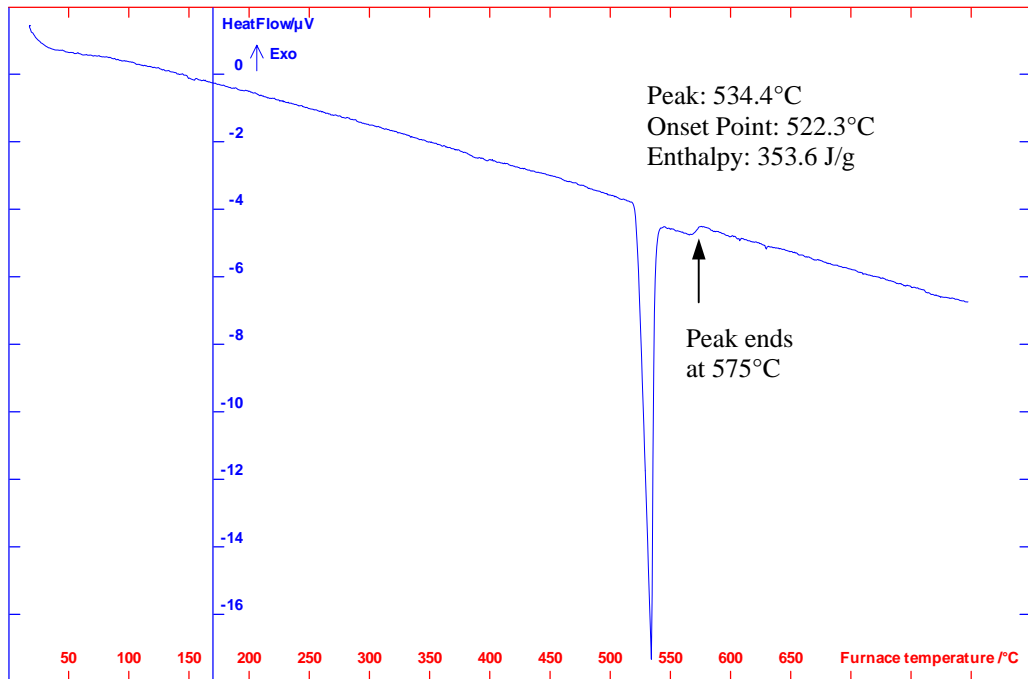


Figure 8: DSC curve of sample 5 with integration of phase change peaks.

DSC spectrum of sample 5 is plotted in Figure 8. It shows one endothermic peak at 522°C. The enthalpy of melting for this sample was registered as 353 J/g. The onset temperature during cooling was about 10°C lower than the onset temperature observed in the heating cycle. This composition is very close to a ternary eutectic point, because the sharp peak is not followed by a shoulder or other heat effect.

Figure 9 shows the DSC spectrum of sample 6. During heating and cooling of this sample a single peak was observed. The sharp peak is not followed by a shoulder, which indicates that this composition, also, very close to another ternary eutectic point. The enthalpy and onset temperature were obtained for this composition without taking baseline subtraction and by using linear plot integration. The enthalpy of melting is registered as 268 J/g.

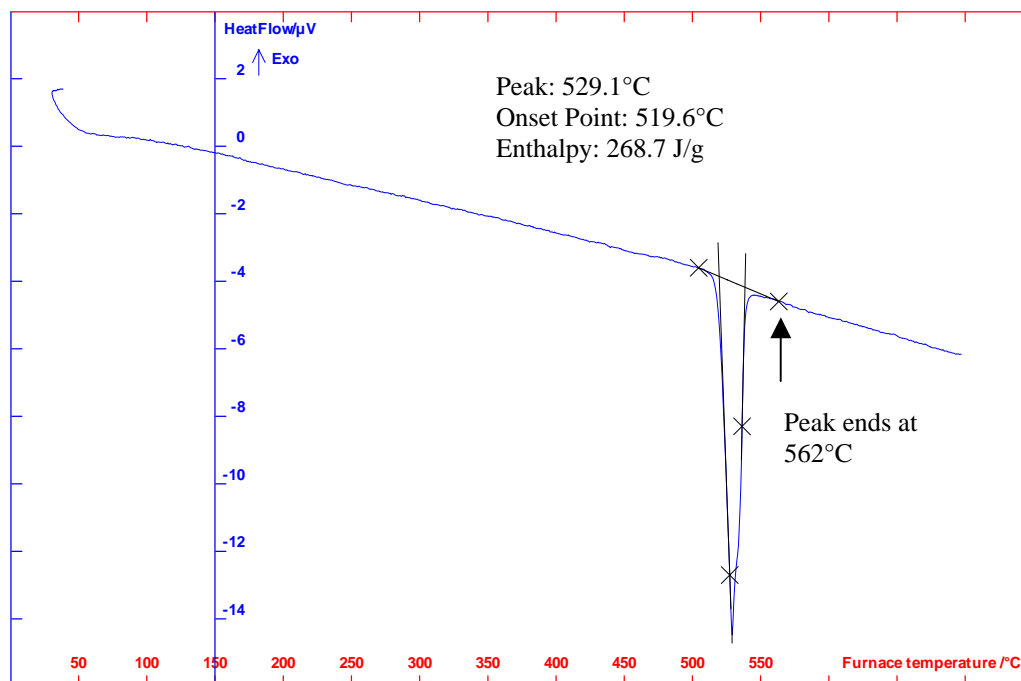


Figure 9: DSC curve of sample 6 with integration of phase change peaks.

DSC spectrum of sample 7 is plotted in Figure 10. It undergoes a phase transition just prior to melting. The onset temperature and enthalpy are calculated after the baseline subtraction. The total values before and after the subtraction are similar. The first peak appeared at 554°C. The peak is sharp and high which indicates the invariant transition. The second peak is non-isothermal transition (univariant) as it exhibits a peak, which is lower and broader. The second peak appears at 628°C. This sample is very close to one of the sample composition reported by Tkachenko *et al.* [8]. Their information is based on the extrapolation of the experimental results of different sample compositions. They reported three phase transformations at 515°C, 550°C and 620°C. Furthermore, the present investigation shows two peaks with onset temperatures, 554°C

and 628°C respectively. The peak ends at 660°C indicating that this is the liquidus temperature for this composition. This discrepancy is probably due to the fact that the values reported by [8] are extrapolations from the thermodynamic model.

Figure 11 shows the DSC spectrum of sample 8. In this sample, the endothermic peak begins at 465°C. The spectrum shows a small peak at 650°C, which however disappeared from the cooling spectrum. This was observed in the three heating/cooling cycles. The temperature corresponds to the tail ends gives the liquidus temperature, which is 800°C.

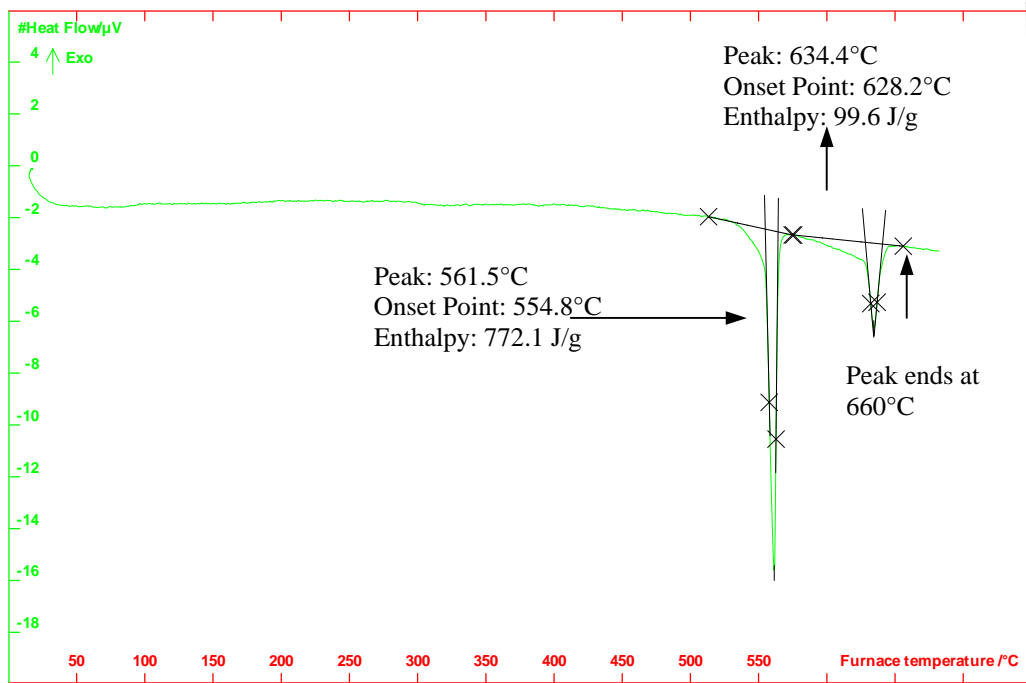


Figure 10: DSC curve of sample 7 with integration of phase change peaks.

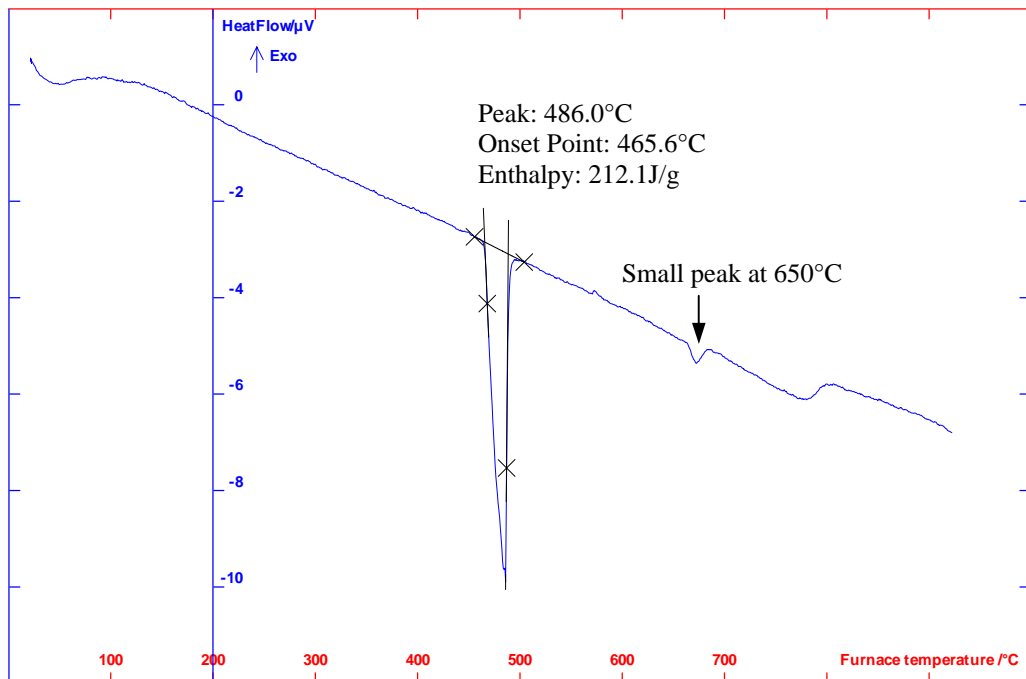


Figure 11: DSC curve of sample 8 with integration of phase change peaks.

4. CONCLUDING REMARKS

The phase diagram of Mg-Al-Ca system was investigated by DSC. The reproducibility of the measured curves is good. A typical error of $\pm 1\%$ was observed between two heating scans. The temperature ranges for the phase changes have been determined. Enthalpy of melting and enthalpy of compound formation is also registered. Comparison with available results in the literature was presented and showed good agreement. Eight samples were discussed in this article. This quantitative analysis along with x-ray diffraction and thermodynamic modeling will be used later to construct a reassessed phase diagram for this highly potential system.

5. ACKNOWLEDGEMENTS

This research was carried out with the support of NATEQ grant, Quebec, Canada. The authors wish to express their appreciation for this support. The authors also are indebted to CANMET-MTL for providing the samples.

6. BIBLIOGRAPHY

[1] Pegguleryuz, M., Baril, E., Labelle, P. and Argo S., Heat Resistant Magnesium Alloys for Power Train Applications, Society of Automotive Engineers, [Special Publication] SP (2001).

[2] Friedrich, H., and Schumann, S. The Use of Magnesium in Cars-Today and in the Future IMA-55, A Global vision for Magnesium, Corronado, CA, USA, 1-7, 1998.

[3] Pegguleryuz, M., Baril, E., Labelle, P., and Argo, D., Magnesium Diecasting Alloy AJ62X with Superior Creep Resistance, Ductility and Diecastability, Proceedings of the Symposium of The Minerals, Metals & Materials Society (TMS), 201-206, 2003

[4] Gröbner, J., Kevorkov, D., Chumak, I. and Schmid-Fetzer, R., Experimental and Thermodynamic Calculation of Ternary Al-Ca-Mg Phase Equilibria, Zeitschrift fuer Metallkunde, 94(9), (2003).

[5] Pegguleryuz, M., Creep Resistance in Mg-Al-Ca Casting Alloys, Proceedings of the Symposium of The Minerals, Metals & Materials Society (TMS), 12-17, 2000.

[6] Koray, O, Zi-Kui, L., and Luo, A.A., Phase Identification and Microanalysis in the Mg-Al-Ca Alloy System, Proceedings of the Symposium of The Minerals, Metals & Materials Society (TMS), 195-200, 2003.

[7] Zhong, Y., Koray, O., Liu, Z.K., and Luo, A., Computational Thermodynamics and Experimental Investigation of the Mg-Al-Ca-Sr Alloys, Proceedings of the Symposium of The Minerals, Metals & Materials Society (TMS), 69-73, 2000.

[8] Tkachenko, V.G., Khoruzhaya, V.G., Meleshevich, K.A., Karpets.M.V., and Frizel, V.V, Phase Equilibria in the Mg-Al-Ca System, Powder Metallurgy and Metal Ceramics, 42(5-6), 2003.

[9] Lindemann, A. Schmidt, J., Todte, M., and Zeuner, T., Thermal analytical investigations of the magnesium alloys AM 60 and AZ 91 including the melting range, Thermochemica Acta, 382(1-2), 2002.